Twenty-first Symposium (International) on Combustion/The Combustion Institute, 1986/pp. 1473–1481

STATISTICAL CALCULATIONS OF SPHERICAL TURBULENT FLAMES

S. B. POPE
Sibley School of Mechanical and Aerospace Engineering
Cornell University, Ithaca, NY 14853

W. K. CHENG
Mechanical Engineering Department
Massachusetts Institute of Technology
Cambridge, MA 02139

Turbulent flame balls can be produced by the spark ignition of a fuel-air mixture in turbulent motion. Calculations of these statistically-spherical flames are reported and compared with the recent data of Hainsworth.[1] The calculations are based on the Monte Carlo solution of a modelled equation for the joint probability density function (pdf) of the velocities and the reaction progress variable. In order to compare the statistical calculations with single experimental realizations, the joint pdf considered is conditioned on the turbulent velocity at the spark. This separates the flame ball's growth from its random convection by the turbulence. Excellent agreement is found between the calculated and measured evolution of the flame ball radius.

1. Introduction

Several experiments[1–4] have been performed on flame balls in homogeneous turbulence. We present model calculations of such flames and compare our results with the recent measurements of Hainsworth[1].

In Hainsworth's experiments, a uniform premixture of methane and air passes through a turbulence-generating perforated plate to produce, ideally, a uniform mean flow of homogeneous, isotropic turbulence. At a distance x_s' downstream of the plate a spark is discharged and a flame kernel forms. Subsequently the flame expands, its surface is distorted by the turbulence, and it is convected downstream. Under the conditions studied[1], high-speed Schlieren movies reveal that the flame ball is approximately spherical, but its surface becomes progressively wrinkled as it evolves. The important experimental conditions are given in Table I.

This flow presents several challenges to statistical models. The problem we focus on is that the center of the flame ball $X(t)$ may be convected (relative to the mean flow) by the turbulence a significant amount compared to its nominal radius $R(t)$. It is emphasized that $X(t)$ is measured in a coordinate system moving with the mean flow, with its origin $(x,t) = (0,0)$ at the spark. Hence in view of the assumed isotropy, the expectation of $X(t)$ is zero:

$$< X(t) > = 0. \tag{1}$$

At early times, the standard derivation of X(t)

$$X'(t) \equiv < X(t) \cdot X(t) >^{1/2}, \tag{2}$$

is approximately $u't$, where u' is the turbulence intensity. Again at early times, the flame propagation is primarily due to laminar processes and hence the radius $R(t)$ is approximately $\dot{R}_\ell t$. Here $R_\ell(t)$ is the radius of a laminar flame ball, and $\dot{R}_\ell$ is its rate of increase. Simple arguments[1] yield

$$\dot{R}_\ell = S_\ell(\rho_u/\rho_b), \tag{3}$$

where S_ℓ is the laminar flame speed and ρ_b and ρ_u are the burnt and unburnt fluid densities. Thus, at early times, $X'(t)$ and $R(t)$ are approximately in proportion to u' and $\dot{R}_\ell$. It may be seen from Table I that these two quantities are about equal.

Why $X'(t)$ being of the same magnitude as $R(t)$ is a problem to a statistical theory is illustrated on Fig. 1, which shows flame balls from three realizations. While the flow is statistically-spherical, it is clear from the figure that such a statistical description captures little of the physics of the essential flame propagation processes.

TABLE I.
Experimental Conditions

Geometry		
perforated plate hole diameter	d	0.64 cm
perforated plate solidity	s	0.61
spark location	x_s'/d	24.1
mean flight time through measuring section	t_{max}	7 ms
Turbulence properties at x_s'		
mean axial flow velocity	U	14.75 m/s
turbulence intensity	u'	1.93 m/s
longitudinal integral scale	L	0.838 cm
dissipation length scale (Eq. 28)	ℓ	1.50 cm
Taylor microscale	λ	0.098 cm
Kolmogorov microscale	η	0.0044 cm
Taylor scale Reynolds number	Re_λ	125
Flame properties		
initial laminar flame kernel radius	$R_\ell(0)$	0.15 cm
typical final turbulent flame radius	$R(t_{max})$	2 cm
Equivalence ratio $\phi = 0.8$		
laminar flame speed	S_ℓ	0.29 m/s
density ratio	ρ_b/ρ_u	0.19
laminar flame ball propagation speed	$\dot{R}_\ell$	1.53 m/s
Equivalence ratio $\phi = 1.1$		
laminar flame speed	S_ℓ	0.43 m/s
density ratio	ρ_b/ρ_u	0.16
laminar flame ball propagation speed	$\dot{R}_\ell$	2.69 m/s

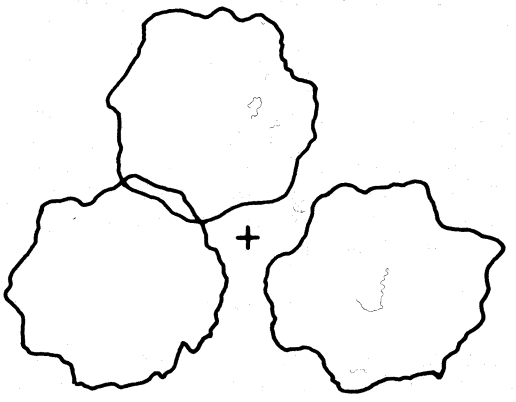

FIG. 1. Flame balls from three realizations shown relative to the spark location (+).

Figure 2 shows the same three flame balls, but this time plotted relative to their respective centers $X(t)$. Because, in this case, there is much more similarity between the flame balls in different realizations, a statistical theory based on this type of representation can be expected to be more successful than one based in absolute coordinates (i.e. Fig. 1).

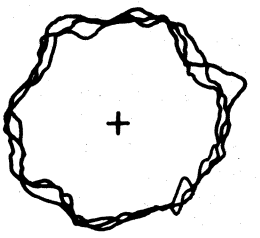

FIG. 2. The three flame balls of Fig. 1 shown relative to their centers (+).

At early times, the position of the flame ball is largely governed by the turbulent velocity $u(x,t)$ prevailing at the spark: that is, (at early times)

$$X(t) \approx u(0,0)t. \tag{4}$$

Consequently, in all realizations with the same "spark velocity" ($u(0,0) = w$, say), the flame balls will have approximately the same center $X(t) \approx wt$, at early times. Thus, following Anand and Pope[5], we adopt an approach in which the statistical quantities are conditioned on the spark velocity.

The conditional pdf method is described in the next section. More than anything else, the conditioning affects the turbulence initial conditions, which are given in section 3. The Monte Carlo solution procedure is briefly described in section 4, and the results are compared to Hainsworth's measurements[1] in section 5.

2. Conditional PDF Method

It is assumed that the thermochemical state of the fluid can be adequately described by a single progress variable $\phi(x,t)$ which is zero in the unburnt reactants and unity in the fully burnt products. (This is the same progress variable—denoted by c—as in the Bray-Moss-Libby model[6].)

The unconditional joint pdf[7] $f(V,\psi;x,t)$ is the probability density of the joint events

$$u(x,t) = V \text{ and } \phi(x,t) = \psi, \tag{5}$$

where V and ψ are independent velocity and composition variables. Prior to the spark the turbulence is homogeneous and isotropic, and $\phi(x,t)$ is zero everywhere. Hence we have

$$f(V,\psi;x,t) = g(V;t)\delta(\psi), \ (t \leq 0), \tag{6}$$

where $g(V;t)$ is an isotropic distribution which, from experiments[8] is known to be Gaussian.

2.1 *Conditional Statistics*

The center of the flame ball (appropriately defined) is denoted by $X(t)$, and its mean conditional upon the spark velocity being w is denoted by $< X(t)|w >$:

$$< X(t)|w > = < X(t)|u(0,0) = w > . \tag{7}$$

The joint pdf of $u(x,t)$ and $\phi(x,t)$ conditional upon $u(0,0) = w$ is denoted by $f_w(V,\psi;y,t|w)$, where $y(w,t)$ is the coordinate relative to the conditional mean flame center:

$$y(w,t) \equiv x - < X(t)|w > . \tag{8}$$

The conditional statistics $<X(t)|w>$ and f_w contain much more information than the unconditional joint pdf which, it may be noted, can be recovered by

$$f(V,\psi;x,t) = \int f_w(V,\psi; < X(t)|w > + y,t|w)g(w;0)dw, \tag{9}$$

where $\int dw$ denotes integration over all values of w.

The conditional pdf depends upon w in two ways: first it is conditional on w; and, second, the coordinate y is relative to $< X(t)|w >$. It is reasonable to assume[5] that the first dependence is weak: that is, all flame balls, when referred to their conditional centers, are statistically similar, depending little on w. Then it is sufficient to know f_w for a single value of w. The obvious choice is zero, since then the conditional mean of $X(t)$ is zero, and f_w is (by symmetry) spherically symmetric. Thus we define

$$f_o(V,\psi;r,t) \equiv f_w(V,\psi;y,t|0), \tag{10}$$

where

$$r^2 = x \cdot x. \tag{11}$$

To summarize: $f_o(V,\psi;r,t)$ is the joint pdf of the velocity $u(x,t)$ and the progress variable $\phi(x,t)$, conditional upon the velocity at the spark being zero. In view of symmetry and the assumed isotropy, f_o depends spatially solely upon the distance r from the spark. It is argued that the statistics of other flame balls ($u(0,0) \neq 0$) are similar when they are referred to their respective centers $< X(t)|w >$. The statistics of the flame ball centers $X(t)$ has been studied by Cheng and Hainsworth[9] and is not considered here.

Since there are large density variations in the flow, it is best to consider the density-weighted conditional pdf

$$\tilde{f}_o(V,\psi;r,t) = \rho(\psi)f_o(V,\psi;r,t)/ < \rho >_o. \tag{12}$$

Here and below, the subscript o indicates a conditional mean:

$$< \rho >_o = < \rho|w = 0 > . \tag{13}$$

The calculations reported here are based on the Monte Carlo solution of a modelled evolution equation for $\tilde{f}_o(V,\psi;r,t)$. In fact, we model the conditional pdf equation in just the same way as the unconditional equation[7]: the conditioning enters through the initial conditions (section 3).

2.2 *Langevin Model*

The modelling of pdf equations is best viewed in terms of notional particles, analogous to fluid particles. Let $x^+(t)$,$u^+(t)$ and $\phi^+(t)$ be the position, velocity and progress variable of a particle. In an infinitesimal time interval dt, x^+changes by

$$dx^+ = u^+(t)dt. \tag{14}$$

The corresponding increments du^+ and $d\phi^+$ are modelled by the Langevin equation[7,10] and by the velocity-biased mixing model (section 2.3).

The Langevin model has been used for several calculations in homogeneous[5,11] and inhomogeneous[12,13] turbulence. The version used here is:

$$du_i^+ = -\left\{\frac{1}{\langle\rho\rangle_0}\frac{\partial\langle p\rangle_0}{\partial x_i}\right\}_{\underline{x}^+} dt$$

$$-(\tfrac{1}{2}+\tfrac{3}{4}C_0)(u_i^+-\tilde{u}_i)\,dt+(C_0\epsilon)^{1/2}\,dW_i. \quad (15)$$

The last two terms together account for the effects of the fluctuating pressure gradient and viscous dissipation[7,10]. The dissipation rate $\epsilon(t)$ and the time scale $\tau(t)$ (defined below Eq. 19) are assumed to be uniform; $C_o = 2.1$ is a universal constant[5]; and $W(t)$ is an isotropic Wiener process:

$$< dW > = 0, \qquad < dW_i dW_j > = dt\ \delta_{ij}. \quad (16)$$

The final term causes the particle to take a random walk in velocity space, while the penultimate term causes a relaxation to the local (unconditional) mean velocity.

Remote from the flame, the turbulent kinetic energy is

$$k(t)\equiv\tfrac{1}{2} < u_i u_i > = \tfrac{3}{2}\,u'(t)^2; \quad (17)$$

the dissipation rate $\epsilon(t)$ is

$$\epsilon(t) = -\frac{dk}{dt}; \quad (18)$$

and the time scale is

$$\tau(t)\equiv k(t)/\epsilon(t). \quad (19)$$

The values of ϵ and τ are determined in the next section and are assumed to be uniform throughout the flow.

The first term on the right-hand side of Eq. (15) represents the effect of the conditional mean pressure gradient:

$$\frac{\partial\langle p\rangle_0}{\partial x_i} \equiv \left\langle \frac{\partial p}{\partial x_i}\,\middle|\,\underline{u}(0,0)=0\right\rangle. \quad (20)$$

In this term the particle density $\rho(\phi^+)$ should be used rather than the conditional mean density $< \rho >_o$. Then the important differential effect of the mean pressure gradient on light and heavy fluid is correctly represented. But this also leads to some numerical problems which, in general, have yet to be solved. (Libby[14] and Anand & Pope[15] have examined the physical effects of the mean pressure gradient in detail.) As a consequence of this shortcoming in Eq. (15), the turbulence levels within the flame ball may not be calculated accurately.

2.3 *Velocity-biased mixing model*

A new model is used to account for the effects of molecular diffusion on the scalar $\phi(x,t)$. Previously, Curl's model[16], or extensions of it[17,18] have been used. The new model can also be viewed as an extension of Curl's model.

Let $(u^{(n)}(t),\phi^{(n)}(t))$ and $(u^{(m)}(t),\ \phi^{(m)}(t))$ be the velocity and composition of two particles at the same physical location. Then in the time interval dt, $\phi^{(n)}(t)$ changes by:

with probability $1-\Theta dt/\tau$:

$$d\phi^{(n)} = 0;$$

with probability $\Theta dt/\tau$: (21)

$$d\phi^{(n)} = \tfrac{1}{2}\alpha[\phi^{(m)}(t)-\phi^{(n)}(t)].$$

Here, Θ is a specified model parameter, and the specification of α distinguishes the different models. For Curl's model[16], α is equal to one: in other models[17,18] α is a random variable, independent of the particle properties ($u^{(n)}$, $u^{(m)}$, $\phi^{(n)}$, $\phi^{(m)}$).

The data of Sirivat & Warhaft[19] provide a good test of mixing models. The data pertain to scalar fluctuations in grid turbulence with an imposed mean scalar gradient. For a given model (i.e. a prescribed distribution of α) the parameter Θ can be chosen so that the model yields the correct scalar variance $< \phi'^2 >$. But, when used in conjunction with the Langevin equation, it is found[7] that the model yields too small a scalar flux $< u_i\phi' >$.

Following a suggestion by Pope[7], the current model overcomes this problem by biasing mixing towards particles (n and m) that have similar velocities. The normalized velocity difference v is defined by

$$v^2 = (u^{(n)}-u^{(m)})\cdot(u^{(n)}-u^{(m)})/u\cdot u, \quad (22)$$

and the mixing parameter α in Eq. (21) is prescribed to be

$$\alpha = \exp(-av^2), \quad (23)$$

where the positive constant a is the bias parameter. Note that if the particle velocities are the same ($v = 0$) then there is complete mixing ($\alpha = 1$). On the other hand, if v^2 is large, α is small and there is little mixing. By reference to Sirivat

& Warhaft's data, the parameter values are found to be[20] $a = 3.9$ and $\Theta = 20$. It may be noted that this value of Θ is about five times greater than that appropriate to Curl's model. (In fact, the selection of particles was based on the improved mixing model algorithm[18]. But, for the results reported below, this is likely to result only in small differences compared to the much simpler model described above.)

2.4 *Reaction*

The treatment of reaction in pdf methods for premixed flames has been discussed by Pope and Anand[21] for both distributed and flame-sheet combustion. The experiments of Hainsworth[1] pertain to the flame-sheet regime.

With little error, reaction in this regime can be treated by "if it's mixed it's burnt". That is, if an initially unburnt particle ($\phi^+(t) = 0$) is mixed to any extent ($\phi^+ > 0$) then it reacts instantly to form products ($\phi^+ = 1$). Thus, in unison with the Bray-Moss-Libby model[6], we obtain a double-delta function distribution for ϕ:

$$f_\phi(\psi) = (1 - < \phi >)\delta(\psi) + < \phi > \delta(1-\psi). \tag{24}$$

And $< \phi(x,t) >$ can be interpreted as the probability of there being products at (x,t).

In the treatment of Pope and Anand[21], it is assumed that the laminar flame speed S_ℓ is negligibly small compared to the turbulence intensity u'. In Hainsworth's experiment S_ℓ is about a fifth of u' (see Table I), but it certainly is not negligible.

An ad hoc method is used to take account of the small but non-negligible laminar flame speed. Let $R_\ell(t)$ be the radius that the flame ball would have if it propagated at the laminar flame speed. Then, any particle lying within the sphere of radius $R_\ell(t)$ is deemed to be fully burnt (i.e. if $x^+(t) < R_\ell(t)$ then $\phi^+(t) = 1$). The value of $R_\ell(t)$ is simply

$$R_\ell(t) = R_\ell(0) + t\,\dot{R}_\ell, \tag{25}$$

where $\dot{R}_\ell$ is given by Eq. (3) and, from the experimental observations, the initial radius is taken to be $R_\ell(0) = 1.5$ mm.

From the models described above it is possible, using standard techniques[7], to derive the modelled evolution equation for $\tilde{f}_o(V,r;t)$. But since the physics of the modelling is most readily understood in terms of the particle evolutions $x^+(t)$, $u^+(t)$, $\phi^+(t)$, the lengthy equation for $\tilde{f}_o(V,r;t)$ is not stated here.

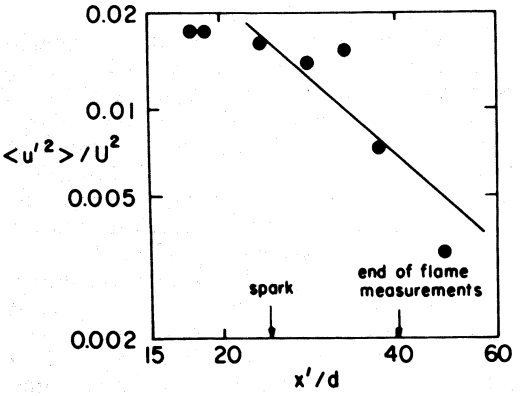

FIG. 3. Decay of velocity variance: measurements of Hainsworth[1]; line is Eq. 26 with $A = 3.18$, $n = 1.643$.

3. Turbulence Properties

The model equations contain the dissipation rate $\epsilon(t)$ and the time scale $\tau(t)$; and initial and boundary conditions are needed for the joint pdf $\tilde{f}_o(V,\psi;r,t)$. The determination of these quantities is described in this section.

Hainsworth[1] measured the axial velocity variance $< u'^2 >$ as a function of distance from the perforated plate x', in the absence of combustion. Figure 3 is a plot of $< u'^2 >$ (normalized by the mean flow velocity U) against x' (normalized by the plate hole diameter d). Turbulence generated by low-solidity grids[8] conforms to the decay law

$$< u'^2 > /U^2 = A(x/d)^{-n}, \tag{26}$$

where A and n are constants and, here, d is the mesh spacing. Figure 3 shows that, in general, Hainsworth's data do not conform closely to such a power law: but within the region of interest (indicated on the figure) there is reasonable agreement with $A = 3.18$, $n = 1.643$. (It is recognized that this value of n is outside the normal range 1.0–1.3. Also, the inclusion of a virtual origin in Eq. 26 does not improve the situation.)

With the assumption of isotropy, from Eq. (26), we can determine the turbulent kinetic energy k, the dissipation rate

$$\epsilon = -U\frac{dk}{dx'}, \tag{27}$$

the length scale

$$\ell \equiv k^{3/2}/\epsilon, \tag{28}$$

and the time scale τ(Eq. 19).

In spite of the scatter in the data evident in Fig. 3, support for the correlation Eq. (26) is provided by the observation that the measured longitudinal integral length scale L divided by ℓ is in the range 0.5–0.7, in good agreement with Comte-Bellot and Corrsin's data[8]. From Eqs. (26–28) other one-point turbulence properties can be determined: some numerical values at the spark location are given in Table I.

Initial conditions on $f_o(V,\psi;r,t)$ are required, or equivalently initial values of the particle properties $u^+(0)$, $\phi^+(0)$. The initial condition on ϕ is readily specified: for $r \le R_\ell(0)$, $\phi = 1$; for $r > R_\ell(0)$, $\phi = 0$. The initial particle velocities $u^+(0)$ are specified to be random vectors with joint pdf $f_c(V;r|u(0) = 0)$. This is the joint pdf of the velocity at r, conditional upon the velocity at $r = 0$ being zero.

The remainder of this section is concerned with modelling f_c. This is achieved by assuming the two-point velocity pdf to be joint normal, and using an empirical equation for the longitudinal correlation function.

For homogeneous isotropic turbulence, $f_2(V,V';r)$ is defined to be the joint pdf of $u(x)$ and $u(x+r)$. With the assumption of Gaussianity, f_2 is completely determined by its means (which are zero) and by the two-point correlations $< u_i(x)u_j(x+r) >$. As is well known[22], in isotropic turbulence all two-point correlations can be determined from the longitudinal correlation

$$h(r) \equiv \langle u_1(x_1,x_2,x_3)u_1(x_1+r,x_2,x_3)\rangle/\langle u_1^2\rangle. \quad (29)$$

Based on the data of Comte-Bellot and Corrsin[8] we use the empirical correlation

$$h(r)=\exp(-1.57[r/\ell]^{3/4}). \quad (30)$$

Thus the two-point pdf $f_2(V,V';r)$ is determined.

Given that f_2 is joint normal it follows that the conditional joint pdf $f_c(V;r)$ is also joint normal. The means of f_c (i.e. $< u(r)|u(0) = 0 >$) are zero. Let u_1 be the velocity in the direction of r, and let u_2 and u_3 be the components normal to r. Then the variances of f_c are

$$< u_1^2 >_o = < u_1(r)^2|u(0) = 0 > = < u_1^2 > (1-h(r)^2), \quad (31)$$

and

$$< u_2^2 >_o = < u_3^2 >_o = < u_1^2 > (1-\bar{h}(r)^2), \quad (32)$$

where $\bar{h}(r)$ is the lateral correlation

$$\bar{h}(r) = h(r) + \frac{1}{2} r \frac{\partial h(r)}{\partial r}. \quad (33)$$

The covariances are zero.

In summary, the initial particle velocity components u_1^+, u_2^+ and u_3^+ are specified to be independent Gaussian random variables with zero means and variances $< u_1^2 >_o$, $< u_2^2 >_o$ and $< u_3^2 >_o$ given by Eqs. (31–32). These variances are plotted on Fig. 4.

(For the present purposes, the above specification of $f_c(V;r)$ is more than adequate. But it should be noted that the two-point pdf f_2 is known not to be joint normal[22], and that the empirical correlation Eq. (30) does not have the correct form at the origin.)

4. Calculation Procedure

The conditional joint pdf equation is solved by a Monte Carlo method[7] in which the joint pdf is represented indirectly by a large number N ($N \approx 20{,}000$) of particles. The *n-th* particle has position $n^{(n)}(t)$, velocity $u^{(n)}(t)$ and progress variable $\phi^{(n)}(t)$. The particles are approximately uniformly distributed in the interval $0 \le r \le r_{max}(t)$.

Hainsworth's measurements show the initial ($t = 0$) laminar flame kernel radius to be $R_\ell(0) = 1.5$ mm; and from Eq. (28) and the given experimental conditions the length scale is $\ell(0) = 1.5$ cm. The initial radius of the solution domain $r_{max}(0)$ was chosen to be the same as $\ell(0)$. Then, the initial flame is well within the solution domain, and the conditional turbulence intensities at $r_{max}(0)$ are close to their unconditional values (see Fig. 4). This greatly facilitates the specification of the turbulence boundary conditions.

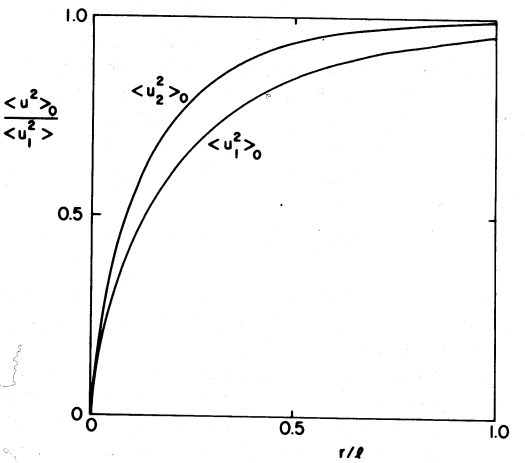

FIG. 4. Conditional velocity variances against radial distance.

The initial particle velocities are independent joint normal random vectors with zero means and variances given by Eqs. (31–32). The progress variable is initially zero ($\phi^{(n)}(0) = 0$) unless the particle is within the flame kernel ($r^{(n)}(0) < R_\ell(0)$), in which case $\phi^{(n)}(0)$ is unity.

The solution is advanced in time through a succession of small time steps. On each step, the particle evolves according to the stochastic equations (Eqs. 15,21). At the center ($r = 0$) symmetry conditions are applied. As the flame grows, the extent of the solution domain $r_{max}(t)$ is increased by the criterion

$$< \phi(r_{max}[t],t) > \leq 0.01. \qquad (34)$$

In order to specify the boundary condition at $r_{max}(t)$, it is assumed that the conditional pdf there is the same as the unconditional pdf in the noncombusting case. Since r_{max}/ℓ is greater than or equal to unity, it is reasonable to assume the conditional and unconditional pdf's to be the same (Fig. 4). The turbulence ahead of the flame suffers some mean distortion due to the flame expansion, but at r_{max} this effect is assumed to be negligible.

Reaction and laminar flame propagation are implemented precisely as they are described in section 2.4.

Mean profiles (e.g. $< \phi(r,t) >$ or $\tilde{\phi}(r,t)$) are extracted from the particle properties by the method of cross-validated cubic smoothing splines[7].

5. Results and Discussion

The principal results reported by Hainsworth[1] are flame-ball radii $R(t)$ as functions of time for two equivalence ratios: $\phi = 0.8$ and $\phi = 1.1$. A Schlieren movie of the flame ball was taken and, for each frame, the outline of the flame ball was digitized. The radius $R(t)$ was then computed as the radius of the circle with the same area as the digitized image.

Because the conditional pdf is a one-point statistical quantity, it is not possible to infer from it the flame radius on a given realization. In fact, since the pdf of ϕ is known to be a double-delta function, the mean $< \phi(r,t) >$ (or $\tilde{\phi}(r,t)$) contains all the information about the flame that can be extracted from the calculations. At a given position the volume-weighted mean $< \phi(r,t) >$ can be interpreted as the probability of the fluid being burnt. The most reasonable statistic to be compared with the measured flame radius would appear then to be $R^*(t)$—which is the radius at which the probability of the fluid being burnt is 0.5: that is

$$< \phi(R^*[t],t) > = \tfrac{1}{2}. \qquad (35)$$

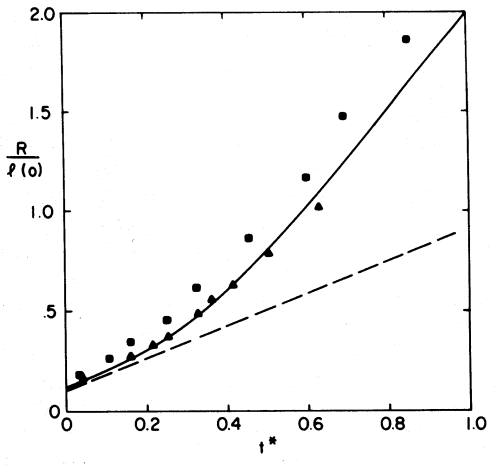

FIG. 5. Flame ball radius versus normalized time: $\phi = 0.8$ solid line—pdf calculation; symbols—different experimental realizations; broken line—radius of laminar flame ball.

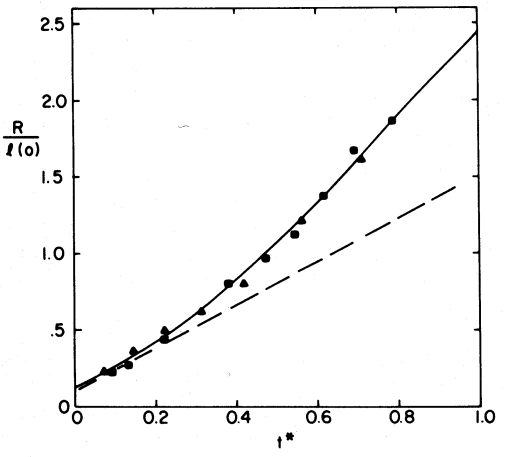

FIG. 6. Flame ball radius versus normalized time: $\phi = 1.1$ solid line—pdf calculation; symbols—different experimental realizations; broken line—radius of laminar flame ball.

For the two equivalence ratios reported by Hainsworth ($\phi = 0.8$ and $\phi = 1.1$), Figs. 5 and 6 show the calculated $R^*(t)$ compared with the measured $R(t)$. The radii are normalized by the initial length scale, while the normalized time is

$$t^* \equiv t\, u'(0)/\ell\,(0). \qquad (36)$$

It may be seen that there is good agreement between the calculations and the measurements.

The slopes of the curves on Figs. (5–6) correspond to the rate of change of radius $\dot{R}(t)$

normalized by the initial turbulence intensity $u'(0)$. The turbulent flame speed is (cf. Eq. 3)

$$S_T = (\rho_b/\rho_u)\,\dot{R}(t). \qquad (37)$$

Initially the turbulent flame speed is equal to the laminar flame speed S_ℓ. But by about 0.3 non-dimensional time units, S_T increases above the laminar value; and between 0.6 and 1.0 time units, S_T appears to have an approximately constant value. Since the turbulence is decaying, a constant value of S_T corresponds to an increasing ratio of S_T to $u'(t)$. For both equivalence ratios, at $t = 1$ the turbulent flame speed is about 3/4 u'. This is significantly less than the values of 1.5 u' and 2.1 u' obtained by Pope and Anand[21] and by Anand & Pope[15] using similar modelling for statistically stationary plane flames. But the result is consistent with the previous observation that the calculated value of S_T increases slowly to attain these asymptotic values.

The present model differs in three ways from that used previously for premixed flames[15,21]: the laminar flame speed is incorporated; the velocity-biased mixing model is used; and, the pdf considered is conditional upon the velocity at the spark. It may be asked: are these three new ingredients essential to produce the good agreement seen on Figs. 5–6? The answer is yes.

The initial ($t^* < 0.2$) propagation is due almost entirely to the laminar flame propagation, because the only other mechanism—convection—is small. This is because at small times and radii the conditional velocities are small.

Compared to Curl's model, the velocity-biased mixing model causes about five times the amount of mixing of particles with the same velocity, but less mixing of particles with significantly different velocities. At small times and radii, the conditional velocities are small. Figure 7 shows the conditional radial turbulence intensity u_1' at $R_\ell(t)$ (i.e. $u_1'(R_\ell(t), t)$) and, for comparison, the value of u_1' at r_{max}. It may be seen that $u'(R_\ell(t),t)$ is very small initially, and hence there is a great deal of mixing. This is essential to the successful calculation of the flame-ball radius $R^*(t)$. Calculations using Curl's model show a much slower propagation rate $\dot{R}^*(t)$.

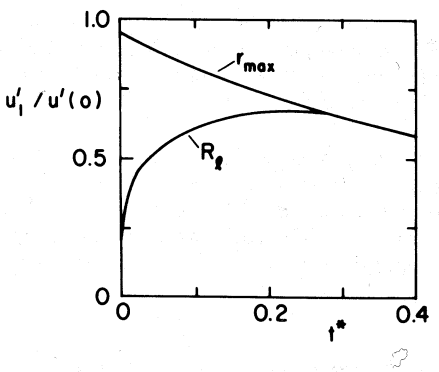

FIG. 7. Conditional radial turbulence intensity u_1' (normalized by initial unconditional intensity) at $R_\ell(t)$ and $r_{max}(t)$ against normalized time.

The use of the pdf conditional upon the velocity at the spark is essential in order to make comparisons with the data, which pertain to individual realizations.

The present modelling and calculations could be improved in two respects. First the differential effect of the mean pressure gradient on burnt and unburnt fluid can be incorporated. Second, a better means of incorporating the laminar flame speed is needed.

Acknowledgement

This work was performed under DOE contract number AC 02-83ER1303A, Dr. Oscar Manley contract manager.

REFERENCES

1. HAINSWORTH, E.: *Study of Free Turbulent Premixed Flames.* M.S. Thesis, M.I.T., 1985.
2. MICKELSON, W.R. AND ERNSTEIN, N.E.: *Sixth Symposium (International) on Combustion,* p. 325, The Combustion Institute, 1956.
3. BOLZ, R.E. AND BURLAGE JR. H.: *Propagation of Free Flames in Laminar and Turbulent Flow Fields,* NASA TND-551, 1960.
4. PALM-LEIS, A. AND STREHLOW, R.A.: *Combust. Flame 13,* 111 (1969).
5. ANAND, M.S. AND POPE, S.B.: in *Turbulent Shear Flows 4,* ed. Bradbury, L.J.S. et al., p. 46, Springer-Verlag, Berlin, 1985.
6. BRAY, K.N.C.: *Turbulent Reactive Flows* (Libby, P.A. and Williams, F.A., Eds.), p. 115, Springer-Verlag, 1980.
7. POPE, S.B.: Prog. Energy Combust. Sci. *11,* 119 (1985).
8. COMTE-BELLOT, G. AND CORRSIN, S.: J. Fluid Mech. *48,* 273 (1971).
9. CHENG, W.K. AND HAINSWORTH E.: *On the Motion of the Center of Mass of a Spherical Turbulent Premixed Flame.* Submitted for publication (1986).
10. POPE, S.B.: Phys. Fluids *26,* 3448 (1983).
11. HAWORTH, D.C. AND POPE, S.B.: Phys. Fluids *29,* 387 (1986).
12. HAWORTH, D.C. AND POPE, S.B.: *Application of a Generalized Langevin Model to the Two-Dimensional*

Mixing Layer, Fifth Symposium on Turbulent Shear Flows, Cornell University (1985).
13. POPE, S.B. AND HAWORTH, D.C.: *The Mixing Layer Between Turbulent Fields of Different Scales. Turbulent Shear Flows 5* (F. Durst et al. Eds.), Springer-Verlag, to be published (1986).
14. LIBBY, P.A.: Prog. Energy Combust. Sci. *11,* 83 (1985).
15. ANAND, M.S. AND POPE, S.B.: *Calculations of Premixed Turbulent Flames by PDF Methods.* Combust. Flame (in press) (1986).
16. CURL, R.L.: A.I.Ch.E.J. *9,* 175 (1963).
17. JANICKA, J., KOLBE, W. AND KOLLMANN, W.: J. Non-equilib. Thermodyn. *4,* 47 (1977).
18. POPE, S.B.: Comb. Sci. Technol. *28,* 131 (1982).
19. SIRIVAT, A. AND WARHAFT, Z.: J. Fluid Mech. *128,* 323 (1981).
20. SONG, J-C.: private communication.
21. POPE, S.B. AND ANAND, M.S.: *Twentieth Symposium (International) on Combustion,* p. 403, The Combustion Institute 1984.
22. HINZE, J.O.: Turbulence, 2nd. ed., Mc-Graw Hill, 1975.

COMMENTS

A. Thomas, University of Liverpool, UK. In your presentation you said that you used no adjustable parameters in your calculations. Can you reassure us that there are no implicitly assumed factors, such as the shape of pdf functions, or the feature of an asymptotically approached turbulent burning velocity as time increases, which could influence the calculation?

Author's Reply. As stated in the presentation, there are no model parameters adjusted to obtain good agreement with premixed flame data. There are, of course, physical parameters such as the laminar flame speed and the turbulence properties that are obtained from the experiments. The model constants C_o, a and θ are determined from experiments on passive scalar transport in grid turbulence.[5,19]

The shape of the joint pdf is not assumed but is calculated from the modelled transport equation. The asymptotic approach to a turbulent burning velocity is an output from the calculation (see ref. 21) not an input to it.

●

Domenic A. Santavicca, Pennsylvania State University, USA. As the flame ball grows its characteristic length scale, i.e. its diameter, changes with time. One would expect that only those turbulent scales which are smaller than the flame ball diameter affect the structure of the flame ball, whereas those turbulence scales which are larger than the flame ball diameter will act to convect the entire flame ball. This latter effect made it necessary in your analysis of the data to redefine the coordinate system to one moving with the center of the flame ball. The turbulence fluctuations which affect the structure of the surface of the flame ball and in turn the rate of growth of the flame ball, however, are only those with scales which are smaller than the growing flame ball diameter. Therefore the turbulence intensity as "seen" by the flame ball varies from a value near zero for flame ball diameter much less than the integral scale of the turbulence to a maximum value when the flame ball diameter is much greater than the integral scale of the turbulence. Do you account for this effect in your calculation?

Author's Reply. The effect you mention is crucial to the flame's development and is certainly accounted for in the calculations. This is most easily seen in the initial conditions: Fig. 4 shows that initially (when the flame ball radius is a tenth of the turbulence scale ℓ) the flame "sees" turbulence with a velocity variance only about 0.35 times the unconditional variance.

●

G. M. Faeth, University of Michigan, USA. The variance of the local flame radius with respect to the mean flame radius is also of interest, since it relates to the turbulent fluctuations of flame position. Have you attempted to measure and predict this variable?

Author's Reply. No. There is a difficulty in relating precisely the measured and calculated quantities to each other. The basic measurement is the flame outline, whereas the calculation is of the probability of finding combustion products at a given radius at a given time. From neither the measurement nor the calculation can the variance of the local flame radius be deduced.